



# Application of solid lipid nanoparticles as a long-term drug delivery platform for intramuscular and subcutaneous administration: *In vitro* and *in vivo* evaluation

Kimberley Elbrink<sup>a,1</sup>, Sofie Van Hees<sup>a,1</sup>, Ronnie Chamanza<sup>b</sup>, Dirk Roelant<sup>c</sup>, Tine Loomans<sup>c</sup>, René Holm<sup>d</sup>, Filip Kiekens<sup>a,\*</sup>

<sup>a</sup> University of Antwerp, Department of Pharmaceutical Technology and Biopharmacy, Universiteitsplein 1, 2610 Wilrijk, Belgium

<sup>b</sup> Janssen Pharmaceutica, Nonclinical Safety, Pathology/Toxicology, Turnhoutseweg 30, 2340 Beerse, Belgium

<sup>c</sup> Janssen Pharmaceutica, Discovery Sciences, DMPK, Turnhoutseweg 30, 2340 Beerse, Belgium

<sup>d</sup> Janssen Pharmaceutica, Drug Product and Development, Parenterals and Liquids, Turnhoutseweg 30, 2340 Beerse, Belgium

## ARTICLE INFO

### Keywords:

Solid lipid nanoparticles  
Intramuscular and subcutaneous administration  
Sustained release  
Pharmacokinetic behavior  
Bedaquiline  
Celecoxib

## ABSTRACT

The purpose of this work was to evaluate solid lipid nanoparticles (SLNs) as a long acting injectable drug delivery platform for intramuscular and subcutaneous administration. SLNs were developed with a low (unsaturated) and high (supersaturated) drug concentration at equivalent lipid doses. The impact of the drug loading as well as the administration route for the SLNs using two model compounds with different physicochemical properties were explored for their *in vitro* and *in vivo* performance. Results revealed that drug concentration had an influence on the particle size and entrapment efficiency of the SLNs and, therefore, indirectly an influence on the  $C_{max}/dose$  and AUC/dose after administration to rats. Furthermore, the *in vitro* drug release was compound specific, and linked to the affinity of the drug compounds towards the lipid matrix and release medium. The pharmacokinetic parameters resulted in an increased  $t_{max}$ ,  $t_{1/2}$  and mean residence time (MRT) for all formulations after intramuscular and subcutaneous dosing, when compared to intravenous administration. Whereas, the subcutaneous injections performed better for those parameters than the intramuscular injections, because of the higher blood perfusion in the muscles compared with the subcutaneous tissues. In conclusion, SLNs extend drug release, need to be optimized for each drug, and are appropriate carriers for the delivery of drugs that require a short-term sustained release in a timely manner.

## 1. Introduction

The development of new drug molecules is an important element of the extended life-expectancies and improved health for humans around the globe. However, the development of new drugs alone is not sufficient to ensure progress in drug therapy in all cases [1]. Currently, long-acting drug release has become an important part of medication with numerous therapeutic advantages, for example, controlled blood levels over time with minimal fluctuation with the potential to provide a significantly improved treatment efficacy [2]. Therefore, the used excipients must provide a release rate of the active pharmaceutical ingredient [3].

The term 'long-acting' was applied in drug delivery to cover the oral

and parenteral applications, but has not been described by a duration of pharmacokinetic exposure. The intention for injectable drug delivery systems is often a therapeutic exposure for weeks to months or even years. The long-acting injectables (LAI) should accomplish at least once a week, once a month, or once every 6-months dosing. Several diseases, such as Human Immunodeficiency Virus and Tuberculosis, require long-term treatment with a risk of failure because of limited patient compliance to the treatment or early discontinuation. Hence, extended-release drug formulations could increase patient adherence and, as a result, improve treatment outcomes and reduce the associated side effects [4–8].

As previously mentioned, long-acting drug delivery covers the oral and parenteral applications, hence the focus of the present work will be

\* Corresponding author at: Universiteitsplein 1, Building A (A.014), 2610 Wilrijk, Belgium.

E-mail addresses: [Kimberley.Elbrink@uantwerpen.be](mailto:Kimberley.Elbrink@uantwerpen.be) (K. Elbrink), [Sofie.VanHees@uantwerpen.be](mailto:Sofie.VanHees@uantwerpen.be) (S. Van Hees), [rchamanz@ITS.JNJ.com](mailto:rchamanz@ITS.JNJ.com) (R. Chamanza), [DROELANT@its.jnj.com](mailto:DROELANT@its.jnj.com) (D. Roelant), [TLOOMANS@its.jnj.com](mailto:TLOOMANS@its.jnj.com) (T. Loomans), [rholm@ITS.JNJ.com](mailto:rholm@ITS.JNJ.com) (R. Holm), [Filip.Kiekens@uantwerpen.be](mailto:Filip.Kiekens@uantwerpen.be) (F. Kiekens).

<sup>1</sup> shared first author

<https://doi.org/10.1016/j.ejpb.2021.04.004>

Received 1 February 2021; Received in revised form 26 March 2021; Accepted 3 April 2021

Available online 10 April 2021

0939-6411/© 2021 Elsevier B.V. All rights reserved.

**Abbreviations**

AUC	Area under the curve	HPLC	High-performance liquid chromatography
BDQ	Bedaquiline	HPLC-UV	High-performance liquid chromatography-ultraviolet
BDQ-S	Bedaquiline supersaturated	LAI	Long-acting injectables
BDQ-U	Bedaquiline unsaturated	MRT	Mean retention time
C <sub>max</sub>	Maximum serum concentration observed	PBS	Phosphate-Buffered Saline
CXB	Celecoxib	RPM	Revolutions per minute
CXB-S	Celecoxib supersaturated	SLNs	Solid lipid nanoparticles
CXB-U	Celecoxib unsaturated	SLS	Sodium lauryl sulfate
DSC	Differential scanning calorimetry	t <sub>1/2</sub>	Half-life
EE	Entrapment efficiency	TFA	Trifluoroacetic acid
F1	Difference factor	t <sub>max</sub>	Time of maximum concentration observed
F2	Similarity factor	UPLC	Ultra Performance Liquid Chromatography
GMS	Glyceryl monostearate	XRPD	X-ray powder diffraction
		ZP	Zeta potential

on two parenteral routes of administration; the intramuscular and subcutaneous routes. Parenteral administration of biodegradable materials, like solid lipids, is a promising drug delivery strategy. Lipids can be incorporated into LAIs to extend the release. Hence, the nanoparticulate systems, such as solid lipid nanoparticles (SLNs), have gained interest [6]. Several advantages of those injection-based parenteral drug delivery systems include the improvement of the solubility of poorly water-soluble compounds and thereby improving the bioavailability, development of parenteral depots, and simplified drug targeting [6]. Thus, the parenteral route is well suited for compounds with small size (needs to be syringed before administration and may impact the safety of the product), low bioavailability, and a very narrow therapeutic index [9,10].

Furthermore, subcutaneously and intramuscularly injections of nanocarriers achieve a reduced systemic penetration due to the dissolution of the compound within the tissue fluids and the passage through the interstitium to reach the blood or lymphatic capillaries [6,11]. It is worth noting that nanocarriers for injection-based delivery have good syringeability and injectability profiles, and the ability to deliver a compound without drastic impact on the viscosity of the system. Therefore, they are good carriers for long-acting locally injectable systems [6,12,13]. Overall, an optimal depot system provides the drug at a predetermined rate within the therapeutic range for a determined duration. For local treatment, drug release at the site of action is desired, or at a systemic level, and with minimal side effects [7].

A potential drug delivery system for lipophilic drugs are solid lipid nanoparticles, which have been designed as exceptionally safe colloidal drug carriers composed of solid lipids, and stabilized by appropriate surfactants. During the manufacturing process, these surfactants are absorbed on the surface of the lipid matrix [14–16]. The main objectives of those particles are associated with their surface properties [17]. SLNs can alter the release profiles of several drugs, e.g. hydrophobic as well as hydrophilic molecules. They can prolong, extend, or sustain the drug's release by retarding its mobility within the solid lipid matrix compared with oil. They protect the drug from degradation, reduce the systemic toxicity of the compound, and improve efficacy by compensating for the drug's release [9,18–22]. Since the drug is incorporated into the SLNs, the type of drug delivery system determines the *in vivo* fate of drugs on parenteral administration rather than the physicochemical properties of the drug [23].

The release rate of the incorporated drug out of the solid lipid nanoparticles has to be taken into account for parenteral drug delivery [24]. The key factors that influenced the latter are the production process (e.g. temperature), the solubility of the drug in the lipid, drug/lipid interactions, the surfactant used, the composition of the lipid matrix, and particle size [16,25]. Furthermore, particle size plays a significant role in the movement of the particles across barriers and penetration

into tissues and organs [26,27].

A plethora of studies showed a difference between drug-loaded and unloaded SLNs. Therefore, the formulation parameters on the physicochemical characteristics of drug-loaded SLNs have to be optimized for each drug [28].

Overall, parenteral depot systems are attractive drug delivery systems which reduce dosing frequency, and improve therapeutic efficacy and patient compliance [7]. In 2010, Bunjes reported that there is only a little experimental evidence that the solid lipid matrix can serve as a platform for the controlled release of a drug. Thus, the pharmacokinetic parameters as well as their relationship to the physical and chemical characteristics of the SLNs should be investigated in more detail [22]. In the meantime more *in vitro* data and reviews were published, while notably, *in vivo* data and the pharmacokinetic behavior of SLNs is still limited for intramuscular and subcutaneous injections.

In this investigation, bedaquiline and celecoxib were used as model drugs with different physicochemical properties. Both drugs are highly lipophilic ( $\log P_{\text{bedaquiline}} 7.25$  [29];  $\log P_{\text{celecoxib}} 3.5$  [30]) and belong to the class II of the biopharmaceutical classification system. The overall aim of this research article was to evaluate SLNs as a long-acting delivery platform, where the delivery mechanism should control the rate of release. Several specific objectives were targeted; a) evaluate the physicochemical properties of the different SLNs formulations; b) compare the *in vivo* release profiles and pharmacokinetic parameters between the supersaturated and unsaturated SLNs for each drug; c) evaluate the differences in release profiles and pharmacokinetic parameters for the different administration routes; and d) determine if the results are compound-specific.

## 2. Materials and methods

### 2.1. Materials

TMC207 (Bedaquiline, free base) was kindly provided by Janssen Pharmaceutica NV (Beerse, Belgium) and Celecoxib was obtained from VWR (Leuven, Belgium). Glyceryl monostearate pure (GMS) and Tween® 80 extra pure were purchased from Carl Roth GmbH (Karlsruhe, Germany). Sodium deoxycholate was acquired from TCI Europe NV (Zwijndrecht, Belgium) and D-Lactose monohydrate was obtained from Sigma-Aldrich Chemie GmbH (Schnellendorf, Germany). The centrifugal filters were purchased from Merck Millipore (Belgium). Acetonitrile HPLC grade and methanol HPLC grade were obtained from Chemlab Analytical BVBA (Belgium). Ammonium acetate was purchased from Acros Organics (Geel, Belgium) and Acetic acid glacial 100% and Trifluoroacetic acid (TFA) from Merck (Darmstadt, Germany). The water used in all experiments was ultrapure water from a Direct pure adept, Replibio Bioscience Ltd., Analis NV (Belgium). The sodium chloride was

purchased from Carl Roth GmbH (Karlsruhe, Germany). Disodium hydrogen phosphate dehydrate was bought from Merck GmbH (Darmstadt, Germany) and potassium phosphate monobasic was purchased from Acros Organics (Geel, Belgium). Sodium lauryl sulfate was bought from Fagron (Nazareth, Belgium) and potassium chloride from Sigma-aldrich Chemie GmbH (Schnelldorf, Germany).

## 2.2. Methods

### 2.2.1. Preparation of solid lipid nanoparticles

**2.2.1.1. Intramuscular and subcutaneous formulations.** The bedaquiline- and celecoxib-SLNs were prepared using high-speed homogenization followed by ultrasonication in an unsaturated and supersaturated formulation. The unsaturated SLNs contained the maximum amount of drug that could be solubilized in the lipid, while the supersaturated SLNs contained more drug than could be dissolved in the lipid matrix (Table 1). The solubility of bedaquiline and celecoxib in the lipid matrix, was 18.35 mg/g and 41.082 mg/g, respectively, determined as described by Patel et al. [31]. For determination of the solubility of the drug in the solid lipid, 5 g of glyceryl monostearate was transferred in a measuring cup maintained at a temperature 5 °C above the melting point of the lipid (56.96 °C). The compound was added in increments until the drug was dissolved. The maximum possible amount of drug being dissolved in the lipid was determined. To manufacture the SLNs, the lipid phase, i.e. glyceryl monostearate, was heated to a temperature 10 °C above the melting point of the selected lipid. The compound was dispersed in the lipid phase, while the aqueous phase was heated to the same temperature. The aqueous solution was prepared by dissolving the surfactants, Tween® 80 extra pure and Sodium deoxycholate, in ultrapure water. Then the heated aqueous phase and heated lipid phase were homogenized by an UltraTurrax® (IKA T18 digital UltraTurrax, Staufen, Germany) at 8000 rpm for 5 min. The obtained o/w emulsion was sonicated by a probe sonicator (Vibra-Cell VCX-750, Sonics, United States) with a 6 mm tapered microtip screwed into the 13 mm threaded end probe at a 20% amplitude for 1 min. The nano-emulsion was placed in an icebox and cooled to room temperature and converted into solid lipid nanoparticles. Cryoprotectant, D-Lactose monohydrate, was added in a 5% (w/w) concentration and the lipid emulsion was vortexed for 3 min. The obtained SLNs dispersions were stored overnight at –20 °C and subsequently freeze-dried for 96 h using a FreeZone 1 Liter Benchtop Freeze Dry System (Model 7740030) (Labconco, MO, USA) at standard conditions (collector temperature of –50 °C and vacuum of 0.133 mBar) [32–34].

**2.2.1.2. Intravenous formulations.** The intravenous formulation was a submicron oil in water emulsion prepared using high-speed stirring followed by ultrasonication (Table 2). The drug, soybean oil and lecithin were mixed and slowly stirred until all components were dissolved at 60 °C. Meanwhile, glycerol and ultrapure water were stirred and heated to the same temperature. The aqueous phase and lipid phase were mixed using the Ultra-Turrax® at 24000 rpm for about 5 min. Thereafter, the O/W emulsion was sonicated with a probe sonicator for 5 min at 40% amplitude. The obtained lipid emulsion was stored at 4 °C.

**Table 1**

Composition of the prepared SLNs-formulations.

Components	Formulation codes				
	BDQ-U	BDQ-S	CXB-U	CXB-S	Blanco
BDQ (mg/g)	1.835	20.000	–	–	–
CXB (mg/g)	–	–	4.108	20.000	–
GMS (g/g)	0.100	0.100	0.100	0.100	0.100
Tween 80 extra pure (g/g)	0.010	0.010	0.010	0.010	0.010
Sodium deoxycholate (g/g)	0.005	0.005	0.005	0.005	0.005
Ultrapure water (g/g)	0.883	0.865	0.881	0.865	0.885

**Table 2**

Composition of the prepared intravenous formulations.

Components	Formulation codes	
	BDQ-IV	CXB-IV
BDQ (mg/g)	5.000	–
CXB (mg/g)	–	1.000
Soybean oil (g/g)	0.200	0.200
Lecithin (g/g)	0.012	0.012
Glycerol (g/g)	0.024	0.020
Ultrapure water (g/g)	0.759	0.767

### 2.2.2. Particle size distribution

Laser light scattering on a Mastersizer 3000 (Malvern, United Kingdom) was used to determine the particle size distribution of the solid lipid nanoparticles, based on the Mie Theory. The SLNs dispersions were added to the sample dispersion unit and the laser obscuration range was set at 2–8%. The samples were measured in triplicate in ultrapure water, using the wet dispersion method.

### 2.2.3. Zeta potential

The zeta potential was measured using a Zetasizer Nano ZS (Malvern, United Kingdom) by dynamic light scattering [35]. The samples were diluted with ultrapure water to avoid multi-scattering phenomena. All measurements were carried out with disposable folded capillary cuvettes. Air bubbles were removed from the capillary before measurements and all formulations were measured in triplicate at a temperature of 25 °C.

### 2.2.4. Entrapment efficiency

Entrapment efficiency (EE) was determined by ultrafiltration [36]. The filter membranes had a molecular weight cut-off of 10 kD and were made of regenerated cellulose. Nanosuspensions were diluted with ultrapure water to a concentration of 5 mg/mL to avoid blocking of the membrane pores. The samples were centrifuged at 14000 × g for 30 min at 20 °C using a centrifuge (3–16 PK, Sigma centrifuges, Germany). The free amount of drug in the supernatant was analyzed with the help of high-performance liquid chromatography (HPLC). EE (%) was calculated by the indirect method (Eq. (1)):

$$EE(\%) = \frac{W_T - W_F}{W_T} \times 100 \quad (1)$$

where  $W_T$  is the total amount of drug and  $W_F$  the amount of free (not included) drug.

### 2.2.5. Differential scanning calorimetry

Thermotropic properties were conducted for bedaquiline, celecoxib, drug-free and drug-loaded SLNs using a Discovery DSC25 equipment (TA Instrument, New Castle, DE, USA). Accurately, 5–10 mg of powders were weighed in Tzero aluminum pans which were sealed. The heat capacity was calibrated using a sapphire standard and an indium standard was used for the calibration of the enthalpy and temperature. Nitrogen gas was purged at a flow rate of 50 mL/min in modulated temperature mode. The samples were heated at a range of –10 °C to 200 °C at a heating rate of 10 °C/min with a modulation of 1.6 °C/min. TA Instruments TRIOS software was used to perform the determination and quantification of the melting peak.

### 2.2.6. X-ray powder diffraction

X-ray powder diffraction (XRPD) analysis was performed on a PANalytical (Philips, Almelo, The Netherlands) X'PertPRO MPO diffractometer with a Cu LFF X-ray tube. The samples were spread on a zero background sample holder and scanned from 3° to 50° 2θ at 45 kV operating voltage and 40 mA current with a step size of 0.02° and a step time of 500 sec/step. The XRPD patterns of the prepared SLNs, bedaquiline, celecoxib, glyceryl monostearate and D-lactose monohydrate

were measured.

### 2.2.7. *In vitro* drug release

The *in vitro* drug release was performed in triplicate for the pure drugs, the bedaquiline-SLNs and the celecoxib-SLNs using a modified USP apparatus 2, with 200 mL phosphate-buffered saline (PBS) pH 7.4  $\pm$  0.1 and 1% (w/V) sodium lauryl sulfate as a dissolution medium at 37  $\pm$  1 °C [37]. Samples were added to the dissolution media and collected at 5, 15, 30, 45, 60, 90, 120, 180, 240, 360 and 1440 min by taking 1 mL of the dissolution medium and immediately replacing it with an equal volume of the fresh release medium. The collected samples were centrifuged at 21000  $\times$  g for 60 min to separate the supernatant from the SLNs and analyzed by HPLC. This set-up is suitable for *in vitro* release testing of drug products and represents sink conditions.

The release profiles of the bedaquiline-SLNs and celecoxib-SLNs were compared with the release profiles of bedaquiline and celecoxib using the difference factor ( $f_1$ ) and the similarity factor ( $f_2$ ). The two curves were considered to be equal if the  $f_1$  value was lower than 15 and the  $f_2$  value above 50 [38]. Additionally, the *in vitro* release data of bedaquiline and celecoxib from SLNs were fitted into the first-order, Higuchi and Weibull equations to study the compound release behavior [43]. According to Costa and Lobo [39], Weibull and Higuchi are the release models that best describe the drug release phenomena [40–42]. The Weibull equation represents the release profiles in terms of relevant parameters. The shape parameter,  $b$ , features the curves as either S-shaped ( $b > 1$ ), exponential ( $b = 1$ ) or as one with a steeper initial slope than consistent with the exponential ( $b < 1$ ). This factor is obtained from the slope of the line and the scale parameter,  $a$ , is estimated from the ordinate value [41,42].

### 2.2.8. Analytical method for the *in vitro* drug release and the entrapment efficiency

The drug content of the samples was measured by HPLC-UV. The HPLC system was equipped with a diode-array detector (Shimadzu SPD-M20A), pump (Shimadzu LC-20AT), auto-sampler (Shimadzu SIL-20A) and degasser (DGu-20A5). Bedaquiline was investigated using a mobile phase composed of methanol/buffer (Ammonium acetate 5 g/L, Acetic acid 25 mL/L, TFA 2 mL/L and ultrapure water) (75:25) and celecoxib of methanol/ultrapure water (75:25). The mobile phase (depending on the drug) was delivered over a reversed-phase C18 column (GraceSmart® RP18 Column 150  $\times$  4.6 mm 5 $\mu$  120A). The flow rate was adjusted to 1 mL/min with an injection volume for each sample of 20  $\mu$ L. The detection wavelength was set at 227 nm for bedaquiline and 250 nm for celecoxib. LC Post-run Analysis (Shimadzu) was used for peak area integration and an external calibration curve for the determination of the concentration.

### 2.2.9. *In vivo* drug release

**2.2.9.1. Animals.** Animal Ethics Committee was in accordance with the local Belgium laws controlling the use of experimental animals as well as EC Directive 2010/63/EU. Pharmacokinetic evaluation was performed in male Sprague Dawley rats supplied by Charles River (Sulzfeld, Germany) with a body weight of 300 to 350 g and age of 9–11 weeks at the start of the study. The rats were group-housed in polysulphon cages with corn cob bedding material, Rodent retreat (Bio-Serv, USA) and Aspen wood block (Datesand, UK) environmental enrichment, and kept in environmentally controlled rooms (humidity range of 30% to 70%, and a temperature range of 20–24 °C) with a 12 h light cycle. They were acclimatized for at least 7 days before the study start and allowed free access to a certified rodent pelleted maintenance diet (SM R/M–Z from SSI NIFF® Spezialdiäten GmbH, Soest, Germany) and tap water during the entire experimental period.

**2.2.9.2. *In vivo* study protocol.** The animals, 33 male rats in total, were

divided into 10 groups (three rats in each group). Groups 1 to 4 received SLNs, namely BDQ-S, BDQ-U, CXB-S, and CXB-U, via intramuscular injection in the left and right hind leg. The same formulations were administered in groups 5 to 8 via subcutaneous injection in the left and right hind leg. Rats from group 9 and 10 received an intravenous injection of 5 mg/mL (bedaquiline) and 1 mg/mL (celecoxib), respectively. Table 3 shows the pharmacokinetic study design in rats. All formulations were administered once on day 1 of the study. Blood samples, 32  $\mu$ L blood, were collected in Vitrex micro hematocrit tubes, by puncture of the tail vein of the rats at appropriately predetermined intervals of time ranging from 0.5 h to 28 days after subcutaneous and intramuscular administration, and from 0.083 h to 24 h after intravenous dosing. After sampling, blood samples were immediately placed on ice and centrifuged at 5 °C, 1500  $\times$  g for approximately 10 min. Then, 10  $\mu$ L plasma aliquots were collected with Vitrex end to end pipettes in FluidX tubes and stored in the freezer until analysis. Pharmacokinetic data were analyzed by non-compartmental analysis (PKSolver®; Microsoft Excel) to calculate the pharmacokinetic parameters. Statistical comparisons were done by the Statistical Package for Social Sciences (SPSS ver. 26.0) using a two-way ANOVA.

### 2.2.9.3. Analysis of the bedaquiline/celecoxib plasma concentration in rats.

Plasma levels of bedaquiline were determined using a liquid chromatography-tandem mass spectrometry (LC-MS/MS) system consisting of a Shimadzu LC30AD HPLC equipment with an SIL-HTC auto-sampler (Shimadzu Scientific Instruments, MD, USA), coupled to an API4000™ triple quadrupole mass spectrometer (AB Sciex, Toronto, Canada) equipped with Turbo Ionspray source operated at 400 °C. Plasma samples were processed by adding subsequently 20  $\mu$ L milli-Q water, 20  $\mu$ L methanol, 20  $\mu$ L internal standard solution and 200  $\mu$ L of ACN to the capillaries in the FluidX tubes. The internal standard solution consisted of 6-deuterium labeled bedaquiline at 100 ng/mL in methanol. After closing, the tubes were shaken horizontally for 10 min on an orbital shaker and centrifuged for 3 min at 2500  $\times$  g. The supernatant (150  $\mu$ L) was transferred to a 96-deepwell plate and 1  $\mu$ L of the sample extracts was injected onto a Waters BEH C18 50  $\times$  2.1 mm, 1.7  $\mu$ m column. Gradient elution was applied for 4 min at a flow rate of 0.6 mL/min using a mobile phase of (A) 0.01 M ammonium formate pH 4.0 and (B) methanol. The percentage of (B) methanol was increased from 65% at time zero to 85% at 3.0 min, to 98% at 3.01 min, kept stable at 98% until 4.0 min, reduced to 65% at 4.01 min and kept stable at 65% until 5 min. Multiple reaction monitoring (MRM) transitions were monitored for bedaquiline (555.2  $\rightarrow$  58  $m/z$ ) and the internal standard (561.2  $\rightarrow$  64  $m/z$ ) applying a collision energy of 71 eV.

The concentration of celecoxib in plasma was determined using UPLC chromatography with MS/MS detection. A quantity of 10  $\mu$ L plasma was mixed with 20  $\mu$ L water, 20  $\mu$ L dimethyl sulfoxide and 200  $\mu$ L of acetonitrile. The samples were centrifuged at 6000  $\times$  g for 20 min at 5 °C. Analysis of the plasma samples was performed by UPLC connected to a tandem mass spectrometer (MS/MS) using a Waters Acquity Ultra Performance Liquid Chromatograph system (Waters Corp.,

**Table 3**  
Pharmacokinetic study design in rats.

Group	N	Formulation	Dosing route	Dosing volume (mL)	Assessments
1	3	BDQ-S	IM	2*0.1	Pharmacokinetics:
2	3	BDQ-U	IM	2*0.1	0–672 h
3	3	CXB-S	IM	2*0.1	Histopathology: Day
4	3	CXB-U	IM	2*0.1	28
5	3	BDQ-S	SC	0.2	
6	3	BDQ-U	SC	0.2	
7	3	CXB-S	SC	0.2	
8	3	CXB-U	SC	0.2	
9	3	BDQ-IV	IV	1 mL/kg	Pharmacokinetics:
10	3	CXB-IV	IV	1 mL/kg	0–24 h

Milford, MA) equipped with a binary solvent delivery system (pump), a sample manager module with autosampler, and a column compartment/heater. A switch valve connected the UPLC to the mass spectrometer. The MS/MS detection was performed using a SCIEX API 4000 MS/MS system with a Turbo Ion Spray® (ESI) as an interface (Applied Biosystems, Carlsbad, CA), operating in the positive ion electrospray mode. Operational settings: celecoxib was detected at a precursor-product ion transition from mass to charge ratio ( $m/z$ ) of 380 to 316. Collision gas (CAD) 6.0, temperature (TEM) 550 °C, IS – 4500 V, entrance potential (EP) – 10.0 V and collision energy (CE) – 30.0 V. For the UPLC analysis, chromatographic separation was performed on a Acquity UPLC BEH C18 (50 × 2.1 mm, 1.7 μm) from Waters Corp. (Milford, MA, USA). The mobile phases contained 0.1% formic acid in water (A) and acetonitrile (B). The total run time was 1.7 min and a gradient system was used. The gradient started at 80.0% A and 20.0% B and was programmed in a linear fashion to 20.0% A and 80.0% B at 1 min. Subsequently the column was cleaned at 90.0% B from 1.1 till 1.3 min. At 1.31 min., conditions changed to initial conditions, viz. 80.0% A and 20.0% B at 1.31 for reconditioning of the column till 1.7 min. The flow rate was 0.60 mL/min. The column temperature was maintained at 40 °C, and the injection volume was 1.0 μL. A lower limit of quantification (LLOQ) and an upper limit of quantification (ULOQ) of 41 and 40,000 ng/mL, respectively, were obtained.

**2.2.9.4. Necropsy and histopathology.** At necropsy, the animals were sacrificed by exsanguination via the carotid artery under isoflurane/oxygen anesthesia, examined grossly, and the following tissues collected and immersed in 10% neutral buffered formalin: the left hind leg containing the intramuscular or subcutaneous administration sites, and the medial iliac and axillary lymph nodes. The tissues were embedded in paraffin wax, sectioned to a 3–4 μm thickness, and stained with hematoxylin and eosin for histopathological evaluation by a qualified pathologist. Histopathological examination was performed for rats from groups 1 to 8. No histopathology analysis was carried out on groups 9 and 10 (intravenous formulations). For each group, one rat was evaluated at the administration site 28 days post-dose. Histopathology analysis was performed on the sampled tissues, namely intramuscular and subcutaneous administration sites, and medial iliac and axillary lymph nodes. A computerized database (Ascentos, Pathology Data Systems Limited, Pratteln, Basel, Switzerland) was used to capture histopathology data and reporting.

### 3. Results and discussion

#### 3.1. Physicochemical characterization of the solid lipid nanoparticles

##### 3.1.1. Particle size, zeta potential, and entrapment efficiency

The results of the median particle size (Dx (50)), zeta potential (ZP) and entrapment efficiency of all the developed SLNs formulations are listed in Table 4. All formulations were in the nanometer range and the particle size distribution was narrow within a range suitable for parenteral use, i.e. below 0.2 μm. The span indices of the formulations were all around 1.3. It was observed that particles containing celecoxib were

**Table 4**

Results of the particle size, zeta potential and entrapment efficiency (n = 3). Statistical comparisons were done with SPSS ver. 26.0 using a two-tailed homoscedastic *t*-test (parametric) or Mann-Whitney test (nonparametric). A *p*-value below 0.05 was statistically significant.

Formulation	Dx(50) (nm)	ZP (mV)	EE (% w/w)
BDQ-S	21.83 ± 3.53	−44.86 ± 3.50	99.01 ± 0.99
BDQ-U	16.67 ± 0.25	−45.99 ± 0.77	98.51 ± 1.12
CXB-S	91.80 ± 0.42	−48.03 ± 5.79	98.49 ± 0.06
CXB-U	41.70 ± 7.78	−46.02 ± 3.94	91.86 ± 1.46
Blanco	17.25 ± 0.21	−53.35 ± 6.48	–

larger than particles containing bedaquiline. The solid lipid nanoparticles had a size below 200 nm, suggesting an increase in the systemic circulation and time for the compound to remain in contact with the target site [44].

The zeta potential is an important parameter to predict the long-term physical stability of the formulations by electrostatic repulsions between the particles. It is optimal to have a zeta potential absolute value >30 mV for stabilization of the SLNs to prevent aggregation of the nanoparticles during storage [45,46]. The formulations investigated in this work all had zeta potentials below −30 mV.

Comparing the values of entrapment efficiency between the two drugs, no significant difference was observed ( $p > 0.05$ ). Both drugs have a high lipophilicity ( $\log P_{\text{bedaquiline}} 7.25$ ;  $\log P_{\text{celecoxib}} 3.5$ ). This was probably driven by the lipophilic nature and the emulsifying properties of the designed matrix, which have been suggested to ensure a high entrapment efficiency [32].

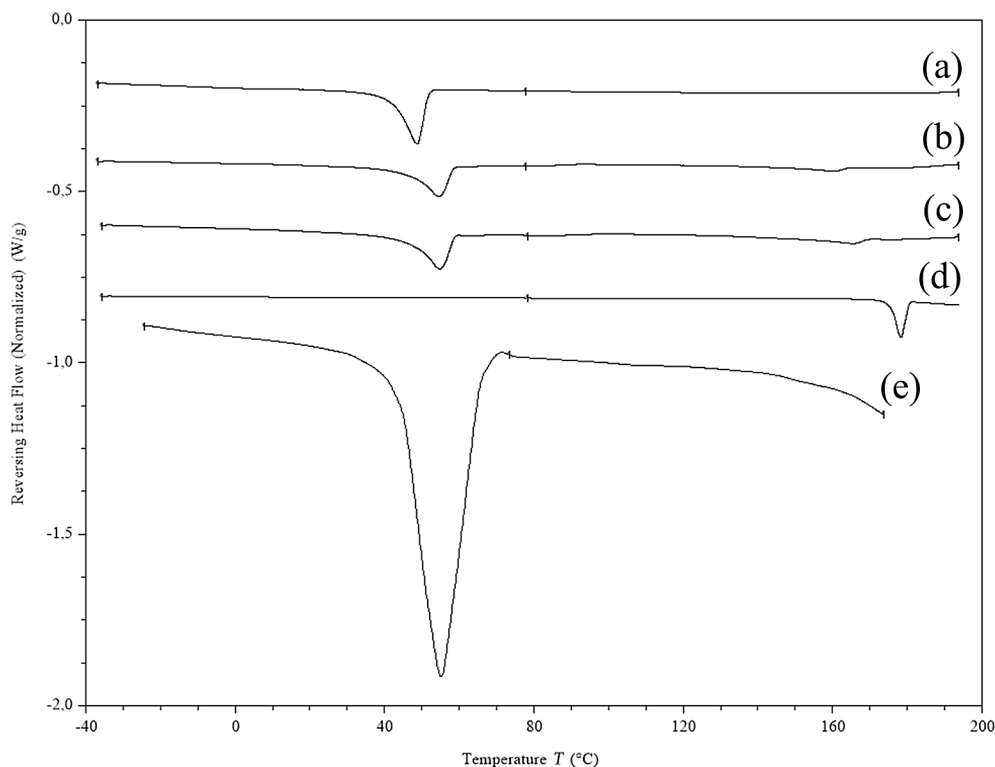
When comparing the nanoparticles with bedaquiline and celecoxib, a significant size difference ( $p = 0.023$ ) was observed between the bedaquiline-SLNs and celecoxib-SLNs. In contrast, no significant difference ( $p > 0.05$ ) was observed in terms of zeta potential and entrapment efficiency.

As mentioned above, particles were made with a low and high drug concentration. Noticeably for the formulations with a high drug concentration, the particles tended to be larger and the entrapment efficiency was higher, though no statistical difference could be detected between size, zeta potential and entrapment efficiency for the different doses of bedaquiline in the SLNs. In contrast, the size ( $p = 0.037$ ) and entrapment efficiency ( $p = 0.001$ ) were significantly different between the low and high drug concentration of celecoxib. Thus, the nature of the drug, and especially the  $\log P$ , may alter the physicochemical properties of the solid lipid nanoparticles [47].

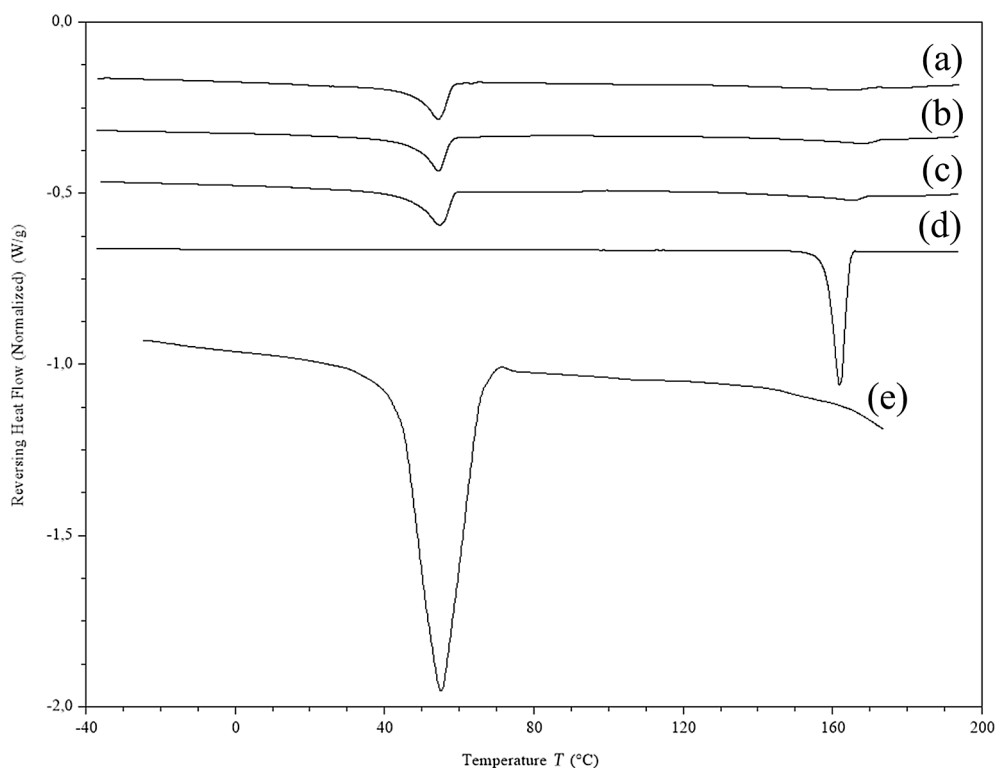
##### 3.1.2. Solid state characterization of the solid lipid nanoparticles

Fig. 1 shows the DSC thermograms of bedaquiline, celecoxib, glyceryl monostearate, D-lactose monohydrate, drug-free SLNs, and drug-loaded SLNs. A sharp endothermic peak was visible at 178.34 °C and 162.32 °C, corresponding to the melting points of pure bedaquiline and celecoxib, as reported in the literature [48,49]. Those peaks refer to the crystalline state of both drugs. Plain glyceryl monostearate displayed a specific melting endothermic peak at 56.96 °C. A shift to a lower temperature ( $\pm 54$  °C) was observed for the blank, bedaquiline- and celecoxib-SLNs, because of their nano-size, i.e. Kelvin effect, the incorporated surfactant in the nanoparticles or the lipid in a dispersed state [32,50–52]. The flattening of this endothermic peak was more pronounced when the drug concentration increased, suggesting an interaction between the drugs and the lipophilic matrix [47]. The DSC thermograms of the bedaquiline- and celecoxib-SLNs lacked the crystalline endothermic peak of the compound, which suggested that the drugs in the SLNs were dissolved or in an amorphous state in all the formulations.

Evaluation of the crystallinity of bedaquiline and celecoxib in the SLNs was done by X-ray powder diffraction. The XRPD patterns of both drugs, the solid lipid (GMS), D-lactose monohydrate, drug-free SLNs, and drug-loaded SLNs were presented in Fig. 2. Plain glyceryl monostearate showed two peaks around 2-theta angles between 18° and 25°, which corresponded with the β-form, as reported in the literature [53,54]. The intensity of those peaks was lower in SLNs than the GMS, suggesting a lower crystallinity of the lipid matrix of solid lipid nanoparticles compared with the bulk material [55]. Sharp crystalline peaks at 2-theta angles around 20° were shown in the diffractogram of D-lactose monohydrate. Crystalline peaks were visible at the diffractogram of pure bedaquiline (Fig 2a), while those characteristic peaks faded away on the XRPD profiles of the bedaquiline-loaded SLNs. In the BDQ-S formulation some small peaks could still be observed, which could be attributed to the drug. Generally, the diffractogram of the SLNs presented peaks corresponding to the drug-free SLNs, which indicated that



**Fig. 1a.** DSC thermograms of BDQ-U (a), BDQ-S (b), drug-free SLNs (c), BDQ (d), and GMS (e).



**Fig. 1b.** DSC thermograms of CXB-U (a), CXB-S (b), drug-free SLNs (c), CXB (d), and GMS (e).

the drug was encapsulated into the nanoparticles, though not fully solubilized/amorphous.

Similar results were determined from the diffraction spectrum of the drug-free and drug-loaded SLNs with celecoxib. The X-ray diffractogram of celecoxib presented intense crystalline peaks at 2-theta angles

between 15° and 30°, which was indicative of the crystalline nature of the compound (Fig 2b) [56]. Again, the CXB-S formulation exhibited some peaks which could be assigned to the drug. This can be explained by the possible presence of celecoxib crystals in the saturated formulation. Overall, the XRPD profiles of the drug-free SLNs and the drug-

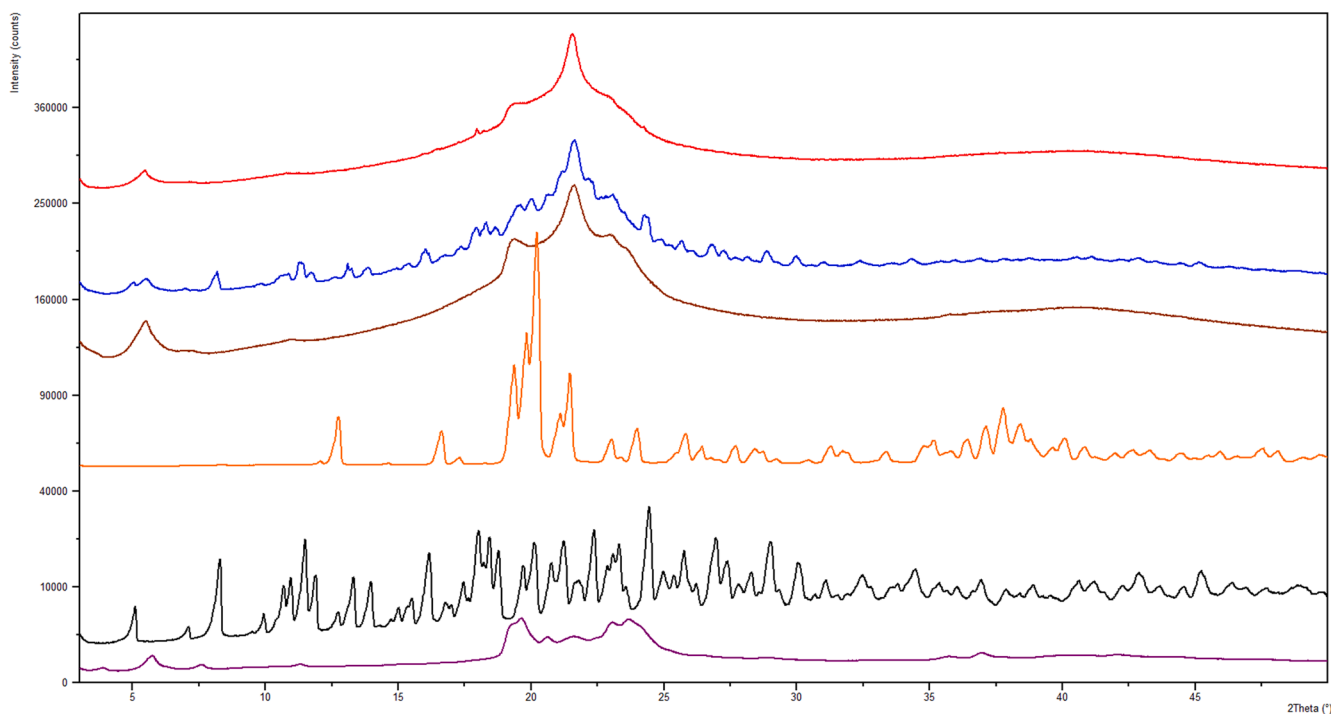


**Fig. 2a.** X-ray powder diffraction patterns of GMS (purple), BDQ (black), D-lactose monohydrate (orange), drug-free SLNs (brown), BDQ-S (blue) and BDQ-U (red).

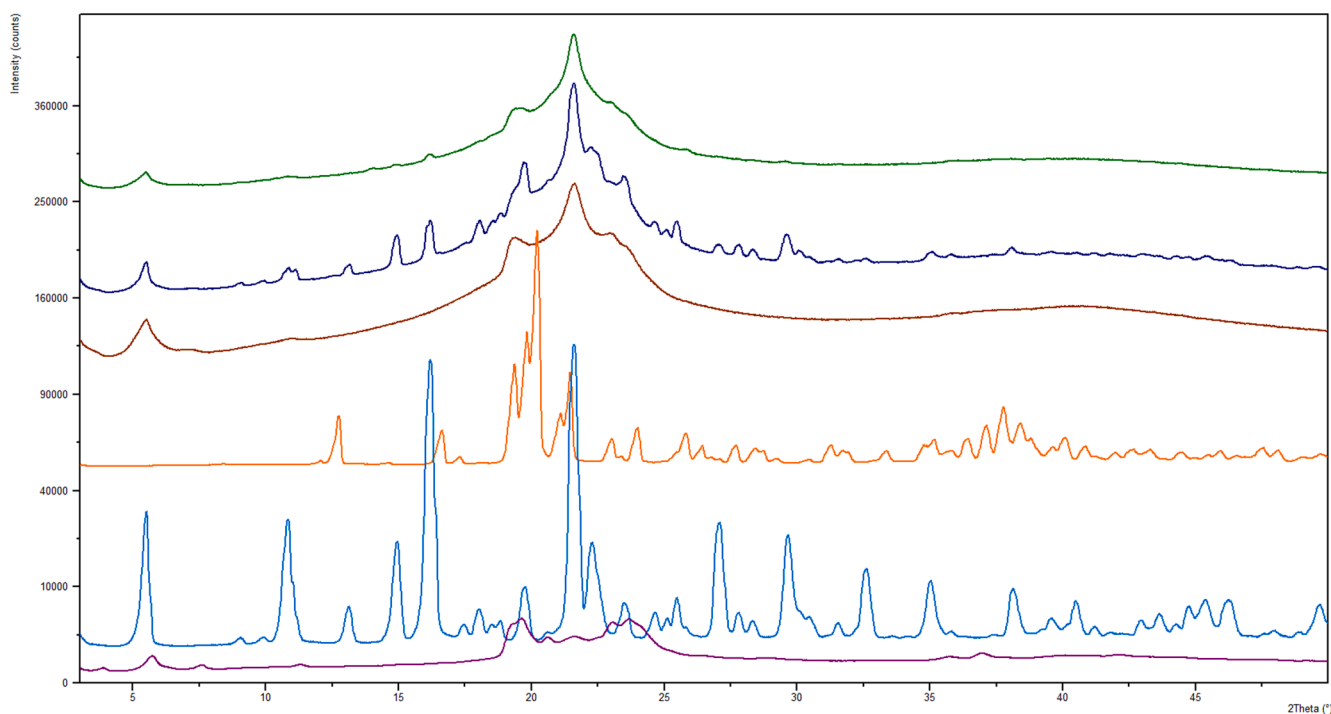


**Fig. 2b.** X-ray powder diffraction patterns of GMS (purple), CXB (light blue), D-lactose monohydrate (orange), drug-free SLNs (brown), CXB-S (dark blue) and CXB-U (green).

loaded SLNs exhibited similar peaks, whereas the drug-loaded SLNs pattern produces a halo, suggesting a fully solubilized/amorphous systems [56].

The crystallinity and the polymorphic form of the lipid matrix has an effect on the drug incorporation and the release profile. The XRPD patterns (Fig 2a and Fig 2b) showed a partially change from the stable  $\beta$ - to the unstable  $\alpha$ -polymorphism during the production of solid lipid nanoparticles. As reported in the literature, the drug release will be

faster from  $\alpha$ , than from  $\beta$  phases [21,57]. Further, the crystallinity of the solid lipid is important for the drug incorporation and an extended release from the carriers. Also, a shift of the endothermic peak of GMS was observed in the DSC thermograms, suggesting a higher drug incorporation due to a more imperfect crystal lattice [16,58,59].

Overall, the data of the characterization of the solid lipid nanoparticles suggested that the manufacturing of solid lipid nanoparticles has some compound dependencies. This might be due to the different

physicochemical properties of both drugs. As mentioned above, bedaquiline has a higher log P than celecoxib. This could explain the higher encapsulation efficiency of bedaquiline in the solid lipid nanoparticles. The size of the celecoxib-loaded SLNs was found to be higher than the bedaquiline-loaded SLNs. With regard to the DSC and XRPD data, the presence of strong drug-lipid interactions was observed, considering the transition from a crystalline to an (partially) amorphous state of the drug [58].

### 3.2. *In vitro* drug release

The *in vitro* drug release was investigated for 24 h, while each sample was analyzed in triplicate. The release profiles of the formulations were compared with both pure drugs, in a phosphate buffer saline solution containing 1% (w/V) sodium lauryl sulfate (SLS). SLS was added to the PBS, as a solubilizing agent, to improve the release of the drug into the medium. Fig 3a shows the percentage release of pure bedaquiline and the SLNs formulations. A burst release was observed for the pure drug and both formulations. Whereas the burst release for the BDQ-U SLNs ( $\pm 70\%$ ) was higher than for the BDQ-S SLNs and the pure drug ( $\pm 15\%$ ). It is our hypothesis that the observed burst release was caused by drug attached to the outside of the particles or drug in the outer shell layer. The obtained results showed that the supersaturated SLNs dispersion of bedaquiline might have crystals of the drug, as it had a release rate similar to the pure bedaquiline. The drug loading played a major role in the drug release of the compounds. The supersaturated formulations had a higher entrapment efficiency than the unsaturated formulations, similar results were obtained by Jansook and coworkers [20]. On the other hand, the results in Fig. 3b present the release profiles of celecoxib and the SLNs formulations. The release patterns of pure celecoxib and the prepared formulations showed no differences. The percentage release of celecoxib was around 80% after one hour. These observations were confirmed by the difference ( $f_1$ ) and similarity factor ( $f_2$ ), which compare the *in vitro* release profiles. Table 5 presents the  $f_1$  and  $f_2$  of all the prepared samples and the drugs as such. The  $f_1$  values and the  $f_2$  values were up to 15 and between 50 and 100 for all the *in vitro* profiles except the BDQ-U formulation. Based on these results, a short-term sustained release was predicted of the SLNs *in vivo* [60]. Although, the  $f_1$  and  $f_2$  equations implement a straightforward manner to express the comparison of the *in vitro* release data, they lack further information on drug release kinetics. Therefore, obtained *in vitro* release data was fitted into the first-order, Higuchi and Weibull equations by the spreadsheet-based nonlinear analysis as described by Juhász et al. [42,61]. The determination coefficients ( $R^2$ ) in Fig. 4 demonstrate that the Weibull model was able to fit all the release data. The shape parameter (Table 6) was  $<1$  for all the different formulations which characterize the curves as profiles with a steeper initial slope than consistent with the exponential. As mentioned above, BDQ-U had a different release profile than

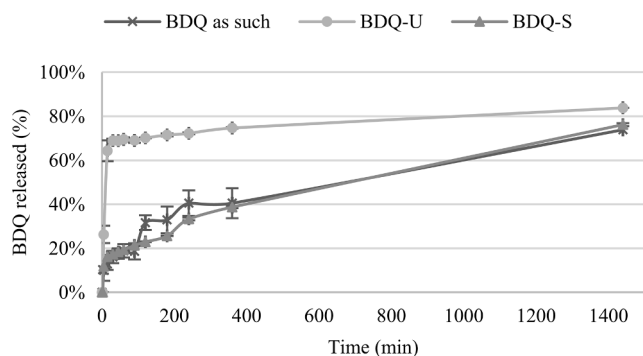


Fig. 3a. *In vitro* release profiles of bedaquiline and the bedaquiline-loaded SLNs formulations in PBS (pH 7.4) + 1% (w/V) SLS at 37 °C. Data are expressed as the mean  $\pm$  SD (n = 3).

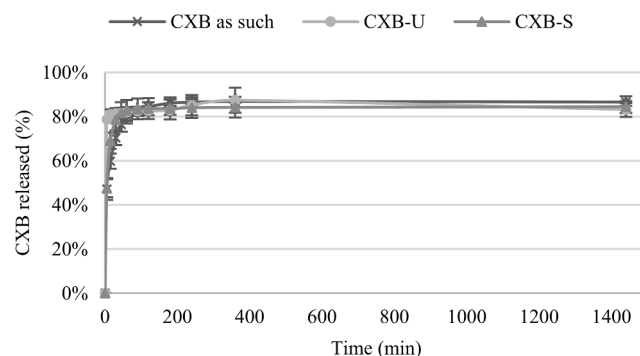


Fig. 3b. *In vitro* release profiles of celecoxib and the celecoxib-loaded SLNs formulations in PBS (pH 7.4) + 1% (w/V) SLS at 37 °C. Data are expressed as the mean  $\pm$  SD (n = 3).

Table 5

*In vitro* drug release - difference and similarity factor.

Formulation	$f_1$ value (%)	$f_2$ value (%)
CXB-S	4.38	67.17
CXB-U	5.92	55.80
BDQ-S	11.76	71.82
BDQ-U	161.03	17.77

BDQ and BDQ-S. This was confirmed by the scale and shape parameter, which were found to be different for BDQ-U compared to BDQ and BDQ-S.

Noteworthy was the difference in drug release profiles between the bedaquiline- and celecoxib-loaded formulations. As discussed above, the drug release from the solid lipid nanoparticles was compound specific. Hence, the drug release patterns will most likely be influenced by the affinity of the drug for the lipid matrix and the release medium [47].

### 3.3. *In vivo* drug release

#### 3.3.1. Pharmacokinetics

Fig. 5 and Table 7 show the mean plasma concentration–time profiles and the associated pharmacokinetic parameters for bedaquiline (Fig. 5a) and celecoxib (Fig. 5b) after intramuscular and subcutaneous administration. The average plasma concentration–time curves for both compounds after intravenous administration are presented in Fig. 6. After intramuscular and subcutaneous administration of celecoxib-loaded SLNs, an initial burst release was observed, followed by a slow-release period. This biphasic release profile can be described by the drug enriched shell model. The initial burst release caused by the drug in the shell was followed by a sustained drug release from the lipid matrix through dissolution and diffusion [16,50]. Similar profiles were recognized after intramuscular and subcutaneous injections of the prepared bedaquiline-SLNs, except for the longer time period of the plasma concentration–time profiles of bedaquiline. The aforementioned difference between the release profiles of the bedaquiline- and celecoxib-loaded SLNs could have been a result of the lower affinity of celecoxib for lipids than bedaquiline, which may have caused the faster release of celecoxib from the SLNs to the blood circulation. Due to the difference between the plasma concentration–time curves for both drugs, it could be concluded that the release of a drug from SLNs was related to the physicochemical properties of the drug itself and the particle size [16,62,63]. When the intramuscular and subcutaneous administration were considered separately,  $C_{max}/\text{dose}$  and  $AUC/\text{dose}$  were significantly different for the two drugs, which was in line with the above observations ( $p < 0.05$ ). These release patterns were desired for prolonged-release products, so the therapeutic drug levels were achieved in time.

The overall profiles of the release curves with celecoxib-loaded SLNs

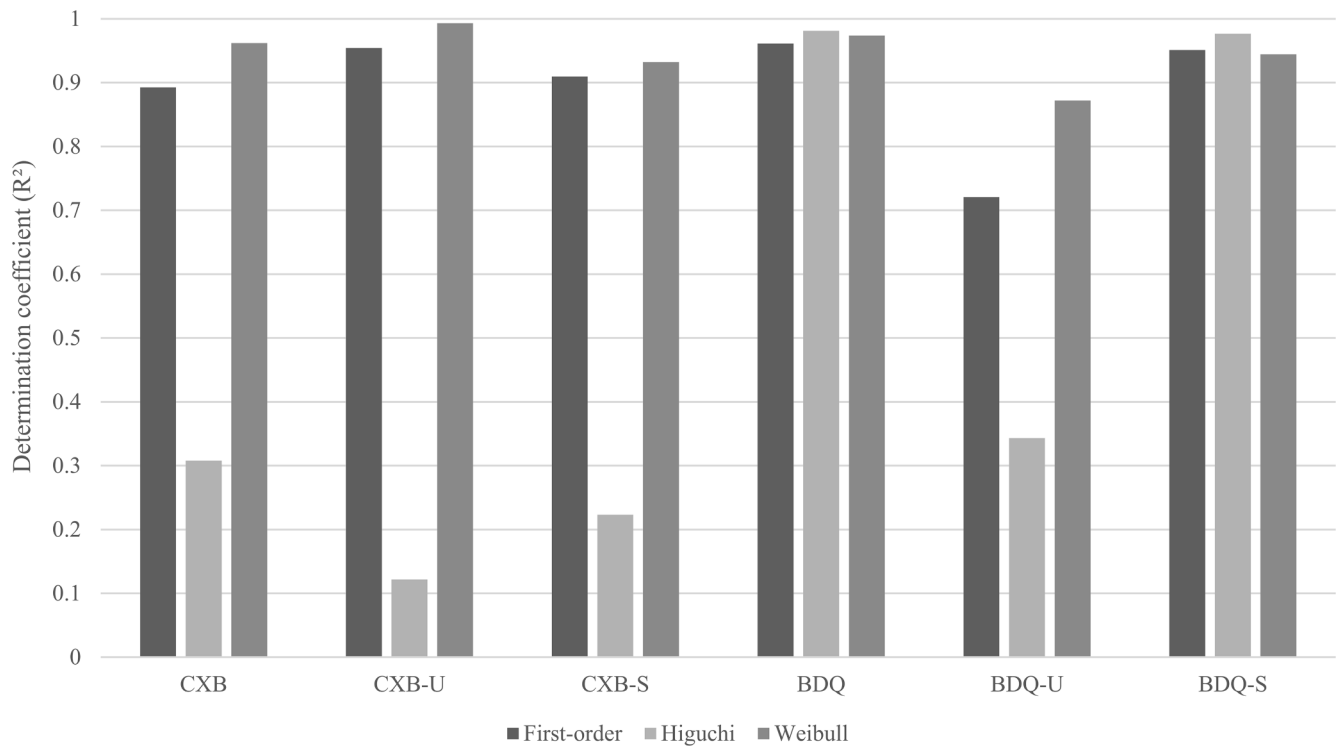


Fig. 4. Comparison of R<sup>2</sup> values qualifying the result of nonlinear dissolution models on different formulations.

Table 6

Parameters of the Weibull model with *a*, scale parameter; *b*, shape parameter; R<sup>2</sup>, determination coefficient.

Dissolution model		CXB	CXB-U	CXB-S	BDQ	BDQ-U	BDQ-S
Weibull	<i>a</i>	0.2224	1.5088	0.3639	0.0015	0.2194	0.0028
	<i>b</i>	0.2215	0.0145	0.1656	0.5839	0.1880	0.5260
	R <sup>2</sup>	0.9620	0.9930	0.9321	0.9737	0.8720	0.9444

Table 7

Pharmacokinetic parameters of bedaquiline and celecoxib in rats following parenteral administration (mean values for n = 3 with SD).

Analyte	Bedaquiline					Celecoxib				
	BDQ-S	BDQ-U	BDQ-S	BDQ-U	BDQ-IV	CXB-S	CXB-U	CXB-S	CXB-U	CXB-IV
Dosing route	IM	IM	SC	SC	IV	IM	IM	SC	SC	IV
Dose (mg/mL)	6	1,2	6	1,2	5	6	3	6	3	1
n	3	3	3	3	3	3	3	3	3	3
C <sub>0</sub> (ng/mL)	–	–	–	–	8827.44 (3227.47)	–	–	–	–	726.87 (177.38)
C <sub>max</sub> (ng/mL)	7.52 (1.21)	8.33 (2.42)	5.55 (1.28)	5.19 (0.92)	5236.67 (1307.15)	234.67 (97.28)	118.47 (39.90)	138.67 (14.57)	136.33 (11.59)	640.33 (125.78)
C <sub>max</sub> /dose (ng/mL)	1.3	6.3	0.7	4.0	905.0	37.8	39.3	23.1	41.3	570.5
t <sub>max</sub> (h)	168	120.00 (83.14)	4.5 (2.12)	216	0	6.67 (2.31)	3.17 (1.44)	8	4 (1.73)	0
t <sub>last</sub> (h)	672	336	672	432	24	216	96	432	216	24
AUC <sub>0-t</sub> (ng.h/mL)	2402.24 (123.37)	1340.77 (184.02)	1792.04 (560.66)	1228.71 (204.58)	7368.46 (1459.44)	9257.72 (1799.53)	4351.68 (951.47)	9868.28 (512.64)	4860.50 (495.17)	2950.10 (410.48)
AUC <sub>0-inf</sub> (ng.h/mL)	2998.58 (211.14)	1564.22 (10.86)	2571.56 (513.71)	1422.12 (185.13)	7667.76 (1679.73)	9808.61 (2019.78)	5112.41 (1360.04)	10051.19 (532.64)	5654.36 (1207.89)	3006.29 (450.72)
AUC/dose (ng.h/mL)	478	1261	454	1158	1483	1573	1599	1643	2621	2770
t <sub>1/2</sub> (h)	264.37 (88.66)	74.09 (15.28)	327.37 (91.87)	115.46 (30.86)	5.78 (0.61)	63.08 (18.52)	30.28 (14.84)	62.27 (4.41)	25.82 (5.64)	4.20 (0.62)
MRT (h)	426.67 (101.68)	152.14 (8.23)	587.98 (102.13)	267.92 (30.88)	5.11 (1.38)	62.47 (12.56)	45.21 (27.62)	85.11 (3.55)	37.44 (9.17)	5.56 (0.92)
F <sub>0-t</sub>	27%	76%	20%	69%	100%	52%	49%	56%	55%	100%
F <sub>0-inf</sub>	33%	85%	28%	77%	100%	54%	57%	56%	63%	100%

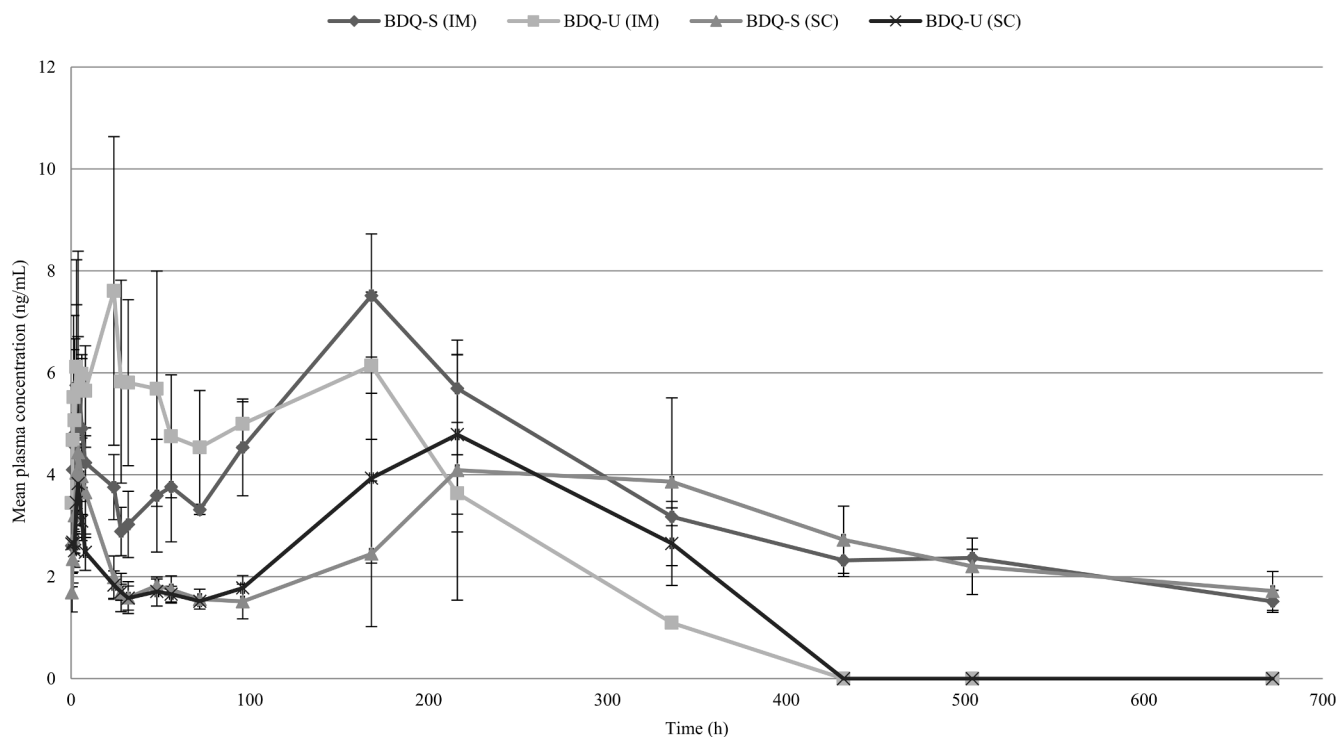


**Fig. 5a.** Plasma concentration–time profiles for the prepared bedaquiline-formulations following intramuscular and subcutaneous injections in rats (mean profiles for  $n = 3$ ). A  $p$ -value below 0.05 was considered statistically significant.

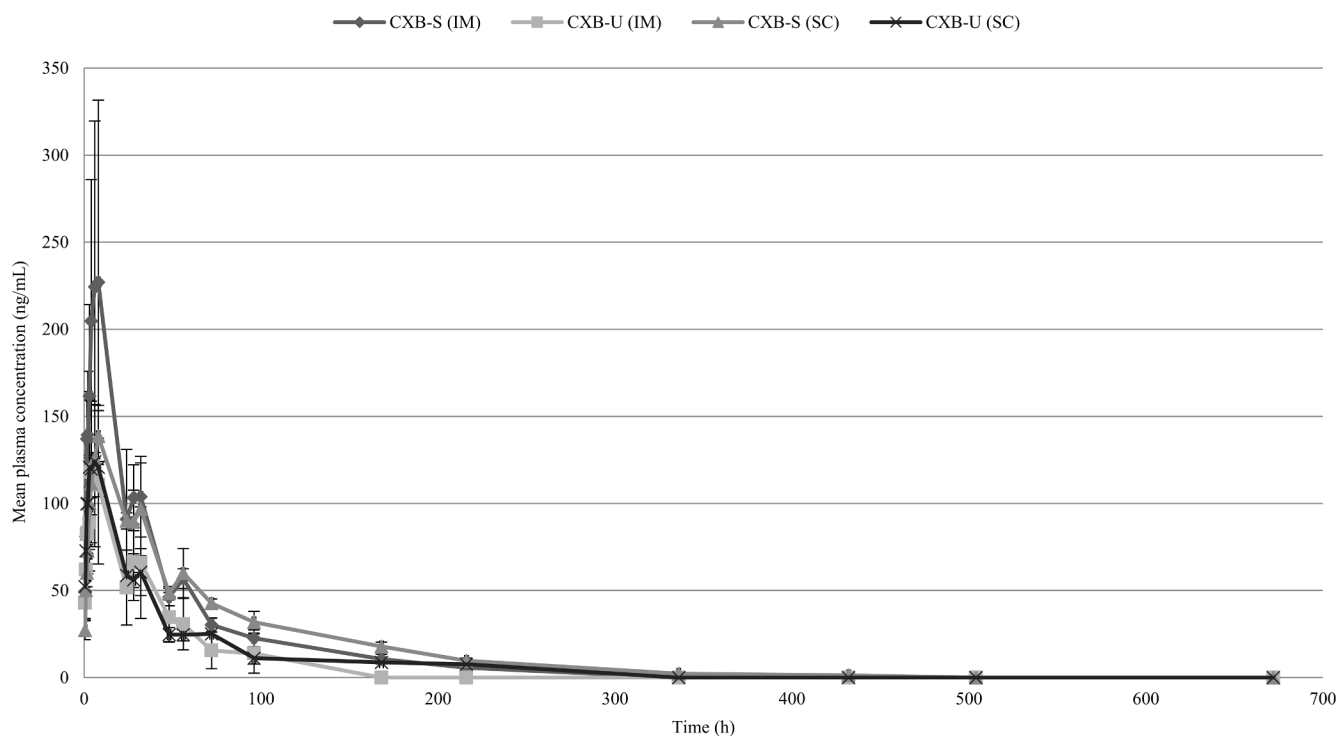


**Fig. 5b.** Plasma concentration–time profiles for the prepared celecoxib-formulations following intramuscular and subcutaneous injections in rats (mean profiles for  $n = 3$ ). A  $p$ -value below 0.05 was considered statistically significant.

showed a burst release followed by a sustained release. The burst release was more prominent for the SLNs loaded with a high concentration of celecoxib than with a low concentration. This could be an indication of the drug deposition in the outer shell layer [64]. After intramuscular and subcutaneous dosing of the celecoxib-loaded preparations, the dose of

the drug encapsulated in the SLNs did not significantly affect the exposure ( $AUC/dose$ ) of the different formulations, neither the  $C_{max}/dose$ ,  $t_{max}$ , mean retention time (MRT) and  $t_{1/2}$  values ( $p > 0.05$ ). Dosing via the intramuscular and subcutaneous route compared with the intravenous route (Fig. 6), resulted in an increased  $t_{max}$ ,  $t_{1/2}$  and MRT,

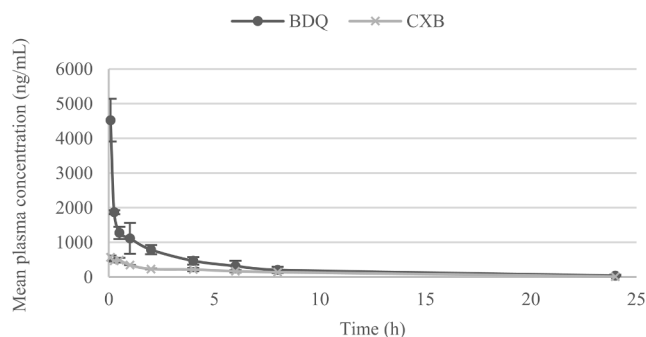


Fig. 6. Plasma concentration versus time curves for the prepared bedaquiline/celecoxib suspensions following intravenous administrations in rats (data are expressed as the mean  $\pm$  SD,  $n = 3$ ). A  $p$ -value below 0.05 was considered statistically significant.

which was statistically confirmed ( $p < 0.05$ ).

The release patterns of formulations loaded with bedaquiline resulted in a biphasic behavior with a rapid drug elimination rate followed by a slow decrease and sustained over 1 ng/mL for 14, 18 and 28 days for BDQ-U (intramuscular), BDQ-U (subcutaneous) and BDQ-S SLNs, indicating their long-acting effect. From this point of view, it could be concluded that the dose of the drug affected the exposure of the drug from the SLNs. This was confirmed by the significant difference of the dose for the  $C_{max}/dose$ ,  $AUC/dose$ , and MRT, whereas no significant effect was determined for the  $t_{max}$  and  $t_{1/2}$ . Compared with the intravenous administration, intramuscular and subcutaneous administration showed higher values for the  $t_{max}$ ,  $t_{1/2}$ , and MRT ( $p < 0.05$ ), the latter due to the flip/flop pharmacokinetics induced by the slow releasing formulation dosed.

The absolute bioavailability ( $F$ ) of the BDQ-U formulation was significantly higher than the BDQ-S formulation after both intramuscular and subcutaneous administration. Less difference was observed in the absolute bioavailability between the different formulations with celecoxib, where no trend nor significant differences were observed. This was in line with the results of the *in vitro* release experiments. Dosing via the intramuscular and subcutaneous route compared with the intravenous route, resulted in an increased  $t_{max}$ ,  $t_{1/2}$  and MRT for all the prepared formulations. The enhanced MRT may be due to the delayed elimination of the drug, because it occurred after the drug was released from the lipid matrix [21]. Comparing the intramuscular and subcutaneous administration, the intramuscular injections of the solid lipid nanoparticles had less effect on the enhancement of pharmacokinetic parameters, such as MRT and  $t_{1/2}$ , than the subcutaneous injections [65]. A possible explanation could be the higher blood perfusion in the muscles compared to the subcutaneous tissues. Therefore, a subcutaneous injection would most likely result in a delayed absorption of the drug [7]. The  $C_{max}/dose$  and  $AUC/dose$  were higher when the unsaturated formulations were injected. A possible explanation could be the differences in the particle size of the SLNs, which were smaller for the unsaturated formulations than the supersaturated ones. Thus, the smaller the drug particle size, the better the *in vivo* performance [66]. The initial burst release may be useful to accomplish a therapeutic drug level, whereas the sustained release could provide the therapeutic concentration *in vivo* [67]. Remarkably, there was an extended exposure of the drug to the body associated with the intravenous administration, potentially lowering the needed dose [68,69].

### 3.3.2. Histopathology

After intramuscular injection at day 28 post dosing, minimal myofiber degeneration and/or fibrosis was found at the administration site. There were no differences in the severity or morphological presentation of the findings at the administration sites between the various formulations or the two test items. Minimal or mild increased cellularity of

lymphoid tissue or histiocytic infiltrates were present in the draining medial iliac lymph nodes. The latter (histiocytic infiltrates) was only observed when the animals were injected intramuscularly with the celecoxib-loaded formulations.

After subcutaneous injection of the formulations, there were no findings at the administration site, although minimal or mild increased cellularity of lymphoid tissue was observed in the draining axillary lymph node, without difference in severity across the groups.

The histopathology results suggest that the intramuscular and subcutaneous administration with the bedaquiline- or celecoxib loaded formulations in male rats was well-tolerated, and not associated with a significant pathology or adverse local reaction. Thus, solid lipid nanoparticles can be used as intramuscularly and subcutaneously carriers, because of their toxicological acceptance and long-term drug delivery to the systemic circulation.

## 4. Conclusion

The observations reported in this work indicated that all formulations had good physicochemical properties, such as a small particle size, sufficient zeta potential and high entrapment efficiency, and were well-tolerated, suggesting that these nanocarriers are suitable for parenteral administration. The different formulations, with a low and high drug concentration, gave different results for the particle size as well as the entrapment efficiency, which did not influence the zeta potential. The pharmacokinetic parameters were enhanced by encapsulating the drugs in the solid lipid nanoparticles. The smaller the particle size, the better the *in vivo* performance. After intramuscular and subcutaneous administration of the SLNs, an extended systemic circulation was observed, due to the gradual release of the incorporated drug from the lipid matrix and the formation of a sustained release depot at the injection sites. The enhanced pharmacokinetic parameters were more pronounced for the subcutaneous injections than the intramuscular injections. Furthermore, the use of compounds with different physicochemical properties has demonstrated that the manufacturing of solid lipid nanoparticles can be influenced by their properties, especially by the log  $P$ . Therefore, the bedaquiline-loaded SLNs showed a longer sustained release of the drug than the celecoxib-loaded SLNs. In conclusion, solid lipid nanoparticles can be optimized according to the physicochemical properties of compounds and utilized as a long-term delivery platform of drugs that require short-term sustained release, such as toxic compounds, after intramuscular and subcutaneous administration.

## Declaration of Competing Interest

The authors declare that they have no known competing financial interests or personal relationships that could have appeared to influence the work reported in this paper.

## Acknowledgments

Many thanks to everyone involved in this research. The authors would like to thank Abhishek Singh for the XRPD patterns.

## References

- [1] W. Mehnert, K. Mäder, Solid lipid nanoparticles: Production, characterization and applications, *Adv. Drug Deliv. Rev.* 64 (2012) 83–101. <https://doi.org/10.1016/j.addr.2012.09.021>.
- [2] H. Ascher-Svanum, D.E. Faries, B. Zhu, F.R. Ernst, M.S. Swartz, J.W. Swanson, Medication adherence and long-term functional outcomes in the treatment of Schizophrenia in usual care, *J. Clin. Psychiatry* 67 (2006) 453–460. <https://doi.org/10.4088/JCP.v67n0317>.
- [3] D. Bikiaris, E. Koutris, E. Karavas, New aspects in sustained drug release formulations, *Recent Pat Drug Deliv Formul.* 1 (2007) 201–213. <https://www.ncbi.nlm.nih.gov/pubmed/19075887>.
- [4] S. Swindells, M. Siccardi, S.E. Barrett, D.B. Olsen, J.A. Grobler, A.T. Podany, E. Nuernberger, P. Kim, C.E. Barry, A. Owen, D. Hazuda, C. Flexner, Long-acting formulations for the treatment of latent tuberculous infection: opportunities and

- challenges, *Int. J. Tuberc. Lung Dis.* 22 (2018) 125–+, <https://doi.org/10.5588/ijtld.17.0486>.
- [5] A. Owen, S. Rannard, Strengths, weaknesses, opportunities and challenges for long acting injectable therapies: Insights for applications in HIV therapy, *Adv. Drug Deliv. Rev.* 103 (2016) 144–156. <https://doi.org/https://doi.org/10.1016/j.addr.2016.02.003>.
- [6] M.A. Shetab Boushehri, D. Dietrich, A. Lamprecht, Nanotechnology as a platform for the development of injectable parenteral formulations: A comprehensive review of the know-hows and state of the art, *Pharmaceutics*. 12 (2020) 1–53, <https://doi.org/10.3390/pharmaceutics12060510>.
- [7] L. Rahnfeld, P. Luciani, Injectable lipid-based depot formulations: Where do we stand? *Pharmaceutics*. 12 (2020) 1–28, <https://doi.org/10.3390/pharmaceutics12060567>.
- [8] C. Flexner, D.L. Thomas, S. Swindells, Creating demand for long-acting formulations for the treatment and prevention of HIV, tuberculosis, and viral hepatitis, *Curr. Opin. HIV AIDS*. 14 (2019) 13–20, <https://doi.org/10.1097/COH.0000000000000510>.
- [9] C. Greve, L. Jorgensen, Therapeutic Delivery, *Ther. Deliv.* 7 (2016) 117–138, <https://doi.org/10.4155/tde.15.92>.
- [10] P.P. Constantinides, M.V. Chaubal, R. Shorr, Advances in lipid nanodispersions for parenteral drug delivery and targeting, *Adv. Drug Deliv. Rev.* 60 (2008) 757–767, <https://doi.org/10.1016/j.addr.2007.10.013>.
- [11] C. Larsen, S.W. Larsen, H. Jensen, A. Yaghmur, J. Østergaard, Role of in vitro release models in formulation development and quality control of parenteral depots, *Expert Opin. Drug Deliv.* 6 (2009) 1283–1295, <https://doi.org/10.1517/17425240903307431>.
- [12] S.P. Schwendeman, R.B. Shah, B.A. Bailey, A.S. Schwendeman, Injectable controlled release depots for large molecules, *J. Control. Release* 90 (2014) 240–253, <https://doi.org/10.1016/j.jconrel.2014.05.057>.
- [13] X.-L. Wei, Y.-R. Han, L.-H. Quan, C.-Y. Liu, Y.-H. Liao, Oily nanosuspension for long-acting intramuscular delivery of curcumin didecanoate prodrug: Preparation, characterization and in vivo evaluation, *Eur. J. Pharm. Sci.* 49 (2013) 286–293, <https://doi.org/10.1016/j.ejps.2013.03.010>.
- [14] J.R. Campos, A.R. Fernandes, R. Sousa, J.F. Fangueiro, P. Boonme, M.L. Garcia, A. M. Silva, B.C. Naveros, E.B. Souto, Optimization of nimesulide-loaded solid lipid nanoparticles (SLN) by factorial design, release profile and cytotoxicity in human Colon adenocarcinoma cell line, *Pharm. Dev. Technol.* 24 (2019) 616–622, <https://doi.org/10.1080/10837450.2018.1549075>.
- [15] S. Doktorovová, A.B. Kovačević, M.L. Garcia, E.B. Souto, Preclinical safety of solid lipid nanoparticles and nanostructured lipid carriers: Current evidence from in vitro and in vivo evaluation, *Eur. J. Pharm. Biopharm.* 108 (2016) 235–252, <https://doi.org/10.1016/j.ejpb.2016.08.001>.
- [16] S.A. Wissing, O. Kayser, R.H. Müller, Solid lipid nanoparticles for parenteral drug delivery, *Adv. Drug Deliv. Rev.* 56 (2004) 1257–1272.
- [17] J.K. Patra, G. Das, L.F. Fraceto, E.V.R. Campos, M.D.P. Rodriguez-Torres, L.S. Acosta-Torres, L.A. Diaz-Torres, R. Grillo, M.K. Swamy, S. Sharma, S. Habtemariam, H.S. Shin, Nano based drug delivery systems: Recent developments and future prospects 10 Technology 1007 Nanotechnology 03 Chemical Sciences 0306 Physical Chemistry (incl. Structural) 03 Chemical Sciences 0303 Macromolecular and Materials Chemistry 11 Medical and He, J. Nanobiotechnology. 16 (2018) 1–33. <https://doi.org/10.1186/s12951-018-0392-8>.
- [18] R. de M. Barbosa, L.N.M. Ribeiro, B.R. Casadei, C.M.G. da Silva, V.A. Queiróz, N. Duran, D.R. de Araújo, P. Severino, E. de Paula, Solid lipid nanoparticles for dibucaine sustained release, *Pharmaceutics*. 10 (2018) 1–17. <https://doi.org/10.3390/pharmaceutics10040231>.
- [19] P. Tyagi, J.A. Subramony, Nanotherapeutics in oral and parenteral drug delivery: Key learnings and future outlooks as we think small, *J. Control. Release* 272 (2018) 159–168, <https://doi.org/10.1016/j.jconrel.2018.01.009>.
- [20] P. Jansook, W. Pichayakorn, G.C. Ritthidej, Amphotericin B-loaded solid lipid nanoparticles (SLNs) and nanostructured lipid carrier (NLCs): effect of drug loading and biopharmaceutical characterizations, *Drug Dev. Ind. Pharm.* 44 (2018) 1693–1700, <https://doi.org/10.1080/03639045.2018.1492606>.
- [21] E.B. Souto, S. Doktorovová, Solid Lipid Nanoparticle Formulations : Pharmacokinetic and Biopharmaceutical Aspects in Drug Delivery, 464 (2009) 105–129. [https://doi.org/10.1016/S0076-6879\(09\)64006-4](https://doi.org/10.1016/S0076-6879(09)64006-4).
- [22] H. Bunjes, Lipid nanoparticles for the delivery of poorly water-soluble drugs, *J. Pharm. Pharmacol.* 62 (2010) 1637–1645, <https://doi.org/10.1111/j.2042-7158.2010.01024.x>.
- [23] M.D. Joshi, R.H. Muller, Lipid nanoparticles for parenteral delivery of actives, *Eur. J. Pharm. Biopharm.* 71 (2009) 161–172, <https://doi.org/10.1016/j.ejpb.2008.09.003>.
- [24] C. Delplace, F. Kreye, D. Klose, F. Danè, M. Descamps, J. Siepmann, F. Siepmann, Impact of the experimental conditions on drug release from parenteral depot systems: From negligible to significant, *Int. J. Pharm.* 432 (2012) 11–22, <https://doi.org/10.1016/j.ijpharm.2012.04.053>.
- [25] K. Sawant, S. Dodiya, Recent Advances and Patents on Solid Lipid Nanoparticles, *Recent Pat. Drug Deliv. Formul.* 2 (2008) 120–135, <https://doi.org/10.2174/187221108784534081>.
- [26] M. Siccardi, P. Martin, D. Smith, P. Curley, T. McDonald, M. Giardiello, N. Liptrott, S. Rannard, A. Owen, Towards a rational design of solid drug nanoparticles with optimised pharmacological properties, *J. Interdiscip. Nanomed.* 1 (2016) 110–123, <https://doi.org/10.1002/jin2.21>.
- [27] D.H. Surve, A.B. Jindal, Recent advances in long-acting nanoformulations for delivery of antiretroviral drugs, *J. Control. Release* 324 (2020) 379–404, <https://doi.org/10.1016/j.jconrel.2020.05.022>.
- [28] S.-J. Lim, C.-K. Kim, Formulation parameters determining the physicochemical characteristics of solid lipid nanoparticles loaded with all-trans retinoic acid, *Int. J. Pharm.* 243 (2002) 135–146, [https://doi.org/10.1016/S0378-5173\(02\)00269-7](https://doi.org/10.1016/S0378-5173(02)00269-7).
- [29] P.J. Choi, H.S. Sutherland, A.S.T. Tong, A. Blaser, S.G. Franzblau, C.B. Cooper, M. U. Lotlikar, A.M. Upton, J. Guillemont, M. Motte, L. Queguiner, K. Andries, W. Van Den Broeck, W.A. Denny, B.D. Palmer, Bioorganic & Medicinal Chemistry Letters Synthesis and evaluation of analogues of the tuberculosis drug bedaquiline containing heterocyclic B-ring units, *Bioorg. Med. Chem. Lett.* 27 (2017) 5190–5196, <https://doi.org/10.1016/j.bmcl.2017.10.042>.
- [30] E. Angela, C.M.O. Driscoll, M. Mcallister, N. Fotaki, European Journal of Pharmaceutical Sciences Gastrointestinal diseases and their impact on drug solubility : Crohn ' s disease, 152 (2020). <https://doi.org/10.1016/j.ejps.2020.105459>.
- [31] K. Patel, S. Padhye, M. Nagarsenker, Duloxetine HCl lipid nanoparticles: preparation, characterization, and dosage form design, *AAPS PharmSciTech.* 13 (2012) 125–133, <https://doi.org/10.1208/s12249-011-9727-6>.
- [32] I.A. Elbahwy, H.M. Ibrahim, H.R. Ismael, A.A. Kasem, Enhancing bioavailability and controlling the release of glicenclamide from optimized solid lipid nanoparticles, *J. Drug Deliv. Sci. Technol.* 38 (2017) 78–89, <https://doi.org/10.1016/j.jddst.2017.02.001>.
- [33] G.A. Shazly, S. Alshehri, M.A. Ibrahim, H.M. Tawfeek, J.A. Razik, Y.A. Hassan, F. Shakeel, Development of Domperidone Solid Lipid Nanoparticles: Vitro and In Vivo Characterization, *AAPS PharmSciTech.* 19 (2018) 1712–1719, <https://doi.org/10.1208/s12249-018-0987-2>.
- [34] G. Abdelbary, R.H. Fahmy, Diazepam-loaded solid lipid nanoparticles: design and characterization, *AAPS PharmSciTech.* 10 (2009) 211–219, <https://doi.org/10.1208/s12249-009-9197-2>.
- [35] R.H. Müller, K. Maeder, S. Gohla, Solid lipid nanoparticles (SLN) for controlled drug delivery—a review of the state of the art, *Eur. J. Pharm. Biopharm.* 50 (2000) 161–177.
- [36] Y. Lv, H. He, J. Qi, Y. Lu, W. Zhao, X. Dong, W. Wu, Visual validation of the measurement of entrapment efficiency of drug nanocarriers, *Int. J. Pharm.* 547 (2018) 395–403, <https://doi.org/10.1016/j.ijpharm.2018.06.025>.
- [37] A. Baán, P. Adriaenssens, J. Lammens, R. Delgado Hernandez, W. Vanden Berghe, L. Pieters, C. Vervae, F. Kiekens, Dry amorphisation of mangiferin, a poorly water-soluble compound, using mesoporous silica, *Eur. J. Pharm. Biopharm.* 141 (2019) 172–179. <https://doi.org/https://doi.org/10.1016/j.ejpb.2019.05.026>.
- [38] J.W. Moore, H.H. Flanner, Mathematical Comparison of Dissolution Profiles, *Pharm. Technol.* 20 (1996) 64–74. <https://www.scopus.com/inward/record.uri?eid=s2-0-2342652446&partnerID=40&md5=cf05d8d4332aaa4571ae4c1ee1f22a93>.
- [39] P. Costa, J.M. Sousa Lobo, Modeling and comparison of dissolution profiles, *Eur. J. Pharm. Sci.* (2001), [https://doi.org/10.1016/S0928-0987\(01\)00095-1](https://doi.org/10.1016/S0928-0987(01)00095-1).
- [40] F. Langenbucher, Letters to the Editor: Linearization of dissolution rate curves by the Weibull distribution, *J. Pharm. Pharmacol.* 24 (1972) 979–981, <https://doi.org/10.1111/j.2042-7158.1972.tb08930.x>.
- [41] L.S. Koester, G.G. Ortega, P. Mayorga, V.L. Bassani, Mathematical evaluation of in vitro release profiles of hydroxypropylmethylcellulose matrix tablets containing carbamazepine associated to  $\beta$ -cyclodextrin, *Eur. J. Pharm. Biopharm.* 58 (2004) 177–179, <https://doi.org/10.1016/j.ejpb.2004.03.017>.
- [42] Á. Juhász, D. Ungor, K. Berta, L. Seres, E. Csapó, Spreadsheet-based nonlinear analysis of in vitro release properties of a model drug from colloidal carriers, *J. Mol. Liq.* 328 (2021), <https://doi.org/10.1016/j.molliq.2021.115405>.
- [43] V. Venkateswarlu, K. Manjunath, Preparation, characterization and in vitro release kinetics of clozapine solid lipid nanoparticles, *J. Control. Release* 95 (2004) 627–638, <https://doi.org/10.1016/j.jconrel.2004.01.005>.
- [44] A. Frank, P. Eric M, L. Robert, F. Omid C, Nanoparticles Technologies for Cancer Therapy, *Handb. Exp. Pharmacol.* 197 (2010) 55–86. <https://doi.org/10.1007/978-3-642-00477-3>.
- [45] A. Gordillo-Galeano, C.E. Mora-Huertas, Solid lipid nanoparticles and nanostructured lipid carriers: A review emphasizing on particle structure and drug release, *Eur. J. Pharm. Biopharm.* 133 (2018) 285–308, <https://doi.org/10.1016/j.ejpb.2018.10.017>.
- [46] S. Das, W.K. Ng, R.B. Tan, Are nanostructured lipid carriers (NLCs) better than solid lipid nanoparticles (SLNs): development, characterizations and comparative evaluations of clotrimazole-loaded SLNs and NLCs? *Eur. J. Pharm. Sci.* 47 (2012) 139–151, <https://doi.org/10.1016/j.ejps.2012.05.010>.
- [47] E. Gué, M. Since, S. Ropars, R. Herbinet, L. Le Pluart, A. Malzert-Fréon, Evaluation of the versatile character of a nanoemulsion formulation, *Int. J. Pharm.* 498 (2016) 49–65, <https://doi.org/10.1016/j.ijpharm.2015.12.010>.
- [48] T. Rawal, S. Patel, S. Butani, Chitosan nanoparticles as a promising approach for pulmonary delivery of bedaquiline, *Eur. J. Pharm. Sci.* 124 (2018) 273–287, <https://doi.org/10.1016/j.ejps.2018.08.038>.
- [49] A.K. Sharma, P.K. Sahoo, D.K. Majumdar, N. Sharma, R.K. Sharma, A. Kumar, Fabrication and evaluation of lipid nanoparticles for ocular delivery of a COX-2 inhibitor, *Drug Deliv.* 23 (2016) 3364–3373, <https://doi.org/10.1080/10717544.2016.1183720>.
- [50] A. zur Muhlen, C. Schwarz, W. Mehnert, Solid lipid nanoparticles (SLN) for controlled drug delivery—drug release and release mechanism, *Eur J Pharm Biopharm.* 45 (1998) 149–155. <https://www.ncbi.nlm.nih.gov/pubmed/9704911>.
- [51] S. Banerjee, S. Roy, K. Nath Bhaumik, P. Kshetrapal, J. Pillai, Comparative study of oral lipid nanoparticle formulations (LNFs) for chemical stabilization of antibiobacterial drugs: physicochemical and cellular evaluation, *Artif. Cells Nanomed. Biotechnol.* 46 (2018) 540–558, <https://doi.org/10.1080/21691401.2018.1431648>.

- [52] K. Shi, Y. Jiang, M. Zhang, Y. Wang, F. Cui, Tocopheryl succinate-based lipid nanospheres for paclitaxel delivery: Preparation, characters, and in vitro release kinetics, *Drug Deliv.* 17 (2010) 1–10, <https://doi.org/10.3109/10717540903431578>.
- [53] V.V. Kumar, D. Chandrasekar, S. Ramakrishna, V. Kishan, Y.M. Rao, P.V. Diwan, Development and evaluation of nitrendipine loaded solid lipid nanoparticles: Influence of wax and glyceride lipids on plasma pharmacokinetics, *Int. J. Pharm.* 335 (2007) 167–175, <https://doi.org/10.1016/j.ijpharm.2006.11.004>.
- [54] R. O'Laughlin, C. Sachs, H. Brittain, E. Cohen, P. Timmins, S. Varia, Effects of Variations in Physicochemical Properties of Glyceryl Monostearate on the Stability of an Oil-in-Water Cream, *J. Soc. Cosmet. Chem.* 40 (1989) 215–229.
- [55] S. Das, W. Kiong, P. Kanaujia, S. Kim, R.B.H. Tan, Colloids and Surfaces B : Biointerfaces Formulation design, preparation and physicochemical characterizations of solid lipid nanoparticles containing a hydrophobic drug : Effects of process variables, *Colloids Surf. B Biointerf.* 88 (2011) 483–489, <https://doi.org/10.1016/j.colsurfb.2011.07.036>.
- [56] Y.H. Liu, C.S. Sun, Y.R. Hao, T.Y. Jiang, L. Zheng, S.L. Wang, Mechanism of Dissolution Enhancement and Bioavailability of Poorly Water Soluble Celecoxib by Preparing Stable Amorphous Nanoparticles, *J. Pharm. Pharm. Sci.* 13 (2010) 589–606, <https://doi.org/10.18433/J3530j>.
- [57] S. Gejage, J. Pawar, P. Amin, Influence of Different Meltable Binders on the Solid-State Behaviour and Dissolution Profiles of Solid Lipid Extrudates Processed Via Continuous Hot Melt Granulation, (2018) 1–27. <https://doi.org/10.20944/preprints201807.0395.v1>.
- [58] O.S. Qureshi, H.S. Kim, A. Zeb, J.S. Choi, H.S. Kim, J.E. Kwon, M.S. Kim, J.H. Kang, C. Ryou, J.S. Park, J.K. Kim, Sustained release docetaxel-incorporated lipid nanoparticles with improved pharmacokinetics for oral and parenteral administration, *J. Microencapsul.* 34 (2017) 250–261, <https://doi.org/10.1080/02652048.2017.1337247>.
- [59] K. Manjunath, J.S. Reddy, V. Venkateswarlu, Solid Lipid Nanoparticles as Drug Delivery Systems, 27 (2005) 1–20. <https://doi.org/10.1358/mf.2005.27.2.876286>.
- [60] M.K. Lee, S.J. Lim, C.K. Kim, Preparation, characterization and in vitro cytotoxicity of paclitaxel-loaded sterically stabilized solid lipid nanoparticles, *Biomaterials* 28 (2007) 2137–2146, <https://doi.org/10.1016/j.biomaterials.2007.01.014>.
- [61] S. Li, Z. Ji, M. Zou, X. Nie, Y. Shi, G. Cheng, Preparation, characterization, pharmacokinetics and tissue distribution of solid lipid nanoparticles loaded with tetrandrine, *AAPS PharmSciTech.* 12 (2011) 1011–1018, <https://doi.org/10.1208/s12249-011-9665-3>.
- [62] H. Mu, R. Holm, Solid lipid nanocarriers in drug delivery: characterization and design, *Expert Opin. Drug Deliv.* 15 (2018) 771–785, <https://doi.org/10.1080/17425247.2018.1504018>.
- [63] W. Mehnert, K. Mäder, Solid lipid nanoparticles: production, characterization and applications, *Adv. Drug Deliv. Rev.* 47 (2001) 165–196.
- [64] A. Zeb, O.S. Qureshi, H.S. Kim, M.S. Kim, J.H. Kang, J.S. Park, J.K. Kim, High payload itraconazole-incorporated lipid nanoparticles with modulated release property for oral and parenteral administration, *J. Pharm. Pharmacol.* 69 (2017) 955–966, <https://doi.org/10.1111/jphp.12727>.
- [65] S. Xie, B. Pan, M. Wang, L. Zhu, F. Wang, Z. Dong, X. Wang, W. Zhou, Formulation, characterization and pharmacokinetics of praziquantel-loaded hydrogenated castor oil solid lipid nanoparticles, *Nanomedicine* 5 (2010) 693–701, <https://doi.org/10.2217/nnm.10.42>.
- [66] D. Leng, H. Chen, G. Li, M. Guo, Z. Zhu, L. Xu, Y. Wang, Development and comparison of intramuscularly long-acting paliperidone palmitate nanosuspensions with different particle size, *Int. J. Pharm.* 472 (2014) 380–385, <https://doi.org/10.1016/j.ijpharm.2014.05.052>.
- [67] Y. Tao, F. Yang, K. Meng, D. Chen, Y. Yang, K. Zhou, W. Luo, W. Qu, Y. Pan, Z. Yuan, S. Xie, Exploitation of enrofloxacin-loaded docosanoic acid solid lipid nanoparticle suspension as oral and intramuscular sustained release formulations for pig, *Drug Deliv.* 26 (2019) 273–280, <https://doi.org/10.1080/10717544.2019.1580798>.
- [68] L. Wright, S. Rao, N. Thomas, R.A. Boulos, C.A. Prestidge, Ramizol((R)) encapsulation into extended release PLGA micro- and nanoparticle systems for subcutaneous and intramuscular administration: in vitro and in vivo evaluation, *Drug Dev. Ind. Pharm.* 44 (2018) 1451–1457, <https://doi.org/10.1080/03639045.2018.1459676>.
- [69] C. Han, C.M. Qi, B.K. Zhao, J. Cao, S.Y. Xie, S.L. Wang, W.Z. Zhou, Hydrogenated castor oil nanoparticles as carriers for the subcutaneous administration of tilmosin: in vitro and in vivo studies, *J. Vet. Pharmacol. Ther.* 32 (2009) 116–123, <https://doi.org/10.1111/j.1365-2885.2008.01009.x>.